

The Snake’s Beating Heart? A Millisecond Pulsar Binary in the Galactic Center Radio Filament G359.1–0.2

MARCUS E. LOWER,¹ SHI DAI,¹ AND SIMON JOHNSTON¹

¹*Australia Telescope National Facility, CSIRO, Space and Astronomy, PO Box 76, Epping, NSW 1710, Australia*

ABSTRACT

The Galactic Center radio filament G359.0–0.2, often referred to as the “Snake”, displays two notable kinks that cause its linear structure to deviate from running perpendicular to the Galactic plane. Using Murriyang, the 64 m Parkes radio telescope, we conducted a search for pulsars centered on the position of a previously identified compact radio and X-ray source in the major kink. We discovered a millisecond pulsar (MSP), PSR J1744–2946, with a period $P = 8.4$ ms, a dispersion measure of 673.7 ± 0.1 pc cm^{−3} and Faraday rotation measure of 3011 ± 3 rad m^{−2}. Its radio pulses are only moderately scattered due to multi-path propagation through the interstellar medium, with a scattering timescale of 0.87 ± 0.08 ms at 2.6 GHz. The pulsar is bound in a 4.8 hr circular orbit around a $M_c > 0.05 M_\odot$ companion. Our discovery of the first MSP within 1° of the Galactic Center hints at a large population of these objects detectable via high frequency surveys. The potential association with the Snake points toward pulsars as the energy source responsible for illuminating Galactic Center radio filaments.

Keywords: Binary pulsars (153) — Galactic Center (565) — Interstellar filaments (842) — Pulsars (1306)

1. INTRODUCTION

The quest to find pulsars in and around the Galactic Center has proved arduous, and mostly unsuccessful. To date, only a handful of long-period pulsars with high dispersion measures (DMs) have been found in blind searches (Johnston et al. 2006; Deneva et al. 2009) in addition to the magnetar SGR 1745–2900 (Eatough et al. 2013; Rea et al. 2013). Yet there is significant evidence for a substantial population of pulsars that reside in the Galactic Center, both from population analyses (Pfahl & Loeb 2004; Ploeg et al. 2020) and as an explanation for the gamma-ray excess seen by the Fermi satellite (O’Leary et al. 2015; Bartels et al. 2016). In addition, the Galactic Center hosts many supernova remnants and a plethora of other structures. This includes the elongated non-thermal radio filaments which trace out magnetic field lines that run predominately perpendicular to the Galactic plane (see e.g. the spectacular image in Heywood et al. 2022). The exact origins of these filaments and the source of the energetic particles powering their emission is presently unknown, though links have been drawn between these structures and pulsars (Barkov & Lyutikov 2019). This has since been reinforced through the discovery that many filaments

appear to have compact radio sources embedded within them (Yusef-Zadeh et al. 2022).

One of the most prominent of these non-thermal filaments is G359.1–0.2. Also known as the Snake, this filament is 70 pc in length but less than 1 pc wide, runs perpendicular to the Galactic plane and is located less than 1° from the Galactic Center (Gray et al. 1991, 1995). The overall structure of Snake appears to be largely linear apart from the ‘major’ and ‘minor’ kinks. Recently, Yusef-Zadeh et al. (2024) conducted an in-depth study of the Snake with the Very Large Array and MeerKAT in the radio band and Chandra in the X-ray band. Within to the major kink, they identified a point source (G359.13142–0.2000) in both X-ray and radio surrounded by a diffuse structure and a tail-like feature. They postulate that the point source is a neutron star with high spin-down energy (\dot{E}) embedded in a pulsar wind nebula (PWN) and that its fast motion (500-1000 kms^{−1}) through the dense medium produces the tail. The neutron star has therefore burst through the Snake sometime in the recent past causing the kink and (perhaps) energizing the Snake structure.

In this Letter, we report the discovery of PSR J1744–2946, the first millisecond pulsar to be found in the Galactic Center. We identify it as the likely source powering G359.13142–0.2000 and discuss the implications of this discovery.

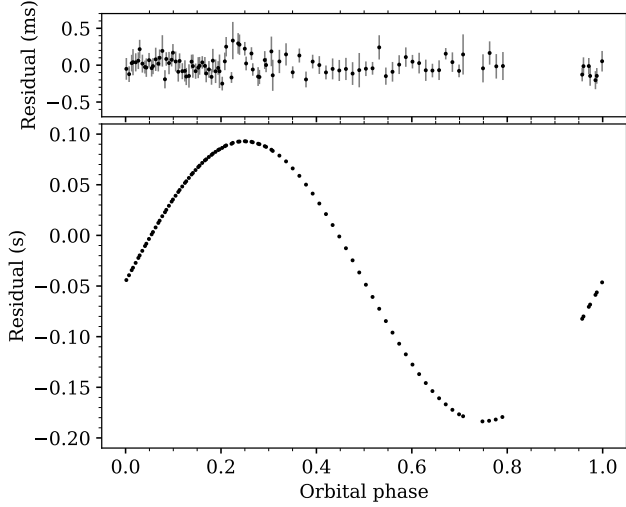


Figure 1. Top panel shows the pulsar timing residuals of PSR J1744–2946 as a function of orbital phase after applying the timing model in Table 1. Bottom panel assumes a binary semi-major axis of zero to demonstrate the influence of the companion object.

2. OBSERVATIONS

We conducted a target of opportunity observation (project code PX130) of G359.13142–0.2000 using the Murriyang Ultra-Wideband Low (UWL) receiver system (Hobbs et al. 2020) on 2024 March 25. A total of 1338 s of 2-bit, total intensity data were recorded using the MEDUSA signal processor, with $512 \mu\text{s}$ sampling and 1 MHz wide frequency channels covering the full 704–4032 MHz band. The resulting filterbank was then searched for periodic dispersed radio signals using the Fourier-domain acceleration search implemented in PRESTO¹ (Ransom 2011) after excising the data below 2.5 GHz, similar to other UWL-based searches for highly scattered pulsars (e.g., Lazarević et al. 2023). We identified a pulsar candidate with a period $P = 8.4 \text{ ms}$ and dispersion measure (DM) of 673 pc cm^{-3} . A large drift in the pulsar period was apparent throughout the observation, indicating the presence of a binary companion. Both the existence of the pulsar, named PSR J1744–2946, and presence of a companion object were confirmed through a second 3600 s duration search-mode observation taken on 2024 April 1, along with 13002 s and 6204 s duration observations taken on 2024 April 3. All three follow-up observations recorded full Stokes search-mode data with $64 \mu\text{s}$ sampling and were coherently dedispersed at the nominal DM of 673 pc cm^{-3} . We also recorded separate calibration observations where the telescope pointing was offset from the pulsar and a switched noise source was injected into the signal chain.

¹ <https://github.com/scottransom/presto>

Table 1. Measured and derived parameters for PSR J1744–2946.

Pulsar parameters	
Right ascension, R.A. (J2000) [†]	17 ^h 44 ^m 19.244 ^s
Declination, Decl. (J2000) [†]	−29°46′52.96″
Spin frequency, ν (Hz)	119.15839530(2)
Epoch (MJD TCB)	60394
Dispersion measure, DM (pc cm^{-3})	673.7(1)
Rotation measure, RM (rad m^{-2})	3011(3)
Solar System ephemeris	DE438
Time span (MJD)	60394–60403
Number of ToAs	100
Flux density at 2.1 GHz, $S_{2.1}$ (mJy)	0.43(4)
Scattering timescale at 2.6 GHz (ms)	0.87(8)
Pulse width, W_{10} (ms)	6.0(1)
Binary model	
Projected semi-major axis, x (lt-s)	0.138196(2)
Epoch of ascending node, T_0 (MJD)	60394.055895(7)
Orbital period, P_b (d)	0.199177(2)
Eccentricity, e	$\lesssim 0.0007$
Spin period, P (ms)	8.392190894(2)
Distance, d (kpc) [*]	8.4
Radio luminosity, $S_2 d^2$ (mJy kpc ²)	30(1)
Mass function, $f(M_p)$ (M_\odot)	0.00007143(3)
Minimum companion mass, M_c^{\min} (M_\odot)	0.0520
Median companion mass, M_c^{med} (M_\odot)	0.0603

Notes. Values in parentheses represent 1σ uncertainties. [†]Position fixed to values from Table 2 of Yusef-Zadeh et al. (2024). ^{*}Distance inferred from the DM and the Cordes & Lazio (2002) model.

To determine the orbital parameters of the system, we used the PREPFOLD function in PRESTO to measure the pulsar spin period in 10-minute segments throughout each observation. The resulting spin period timeseries was then iteratively fit for a circular orbit using FIT_CIRCULAR_ORBIT.PY, which provided estimates of the orbital period, projected semi-major axis, epoch of the ascending node and de-Doppler shifted spin period. We then used our initial timing solution to fold the search-mode data using DSPSR (van Straten & Bailes 2011), averaging the data into 240 s sub-integrations. The folded archives were then flux density and polarization calibrated and cleaned of radio-frequency interference using PSRCHIVE, following the same procedure as Lower et al. (2020).

3. RESULTS

Pulse times of arrival (ToAs) were measured by cross-correlating the frequency-averaged profiles with a noiseless Gaussian template, after which we used TEMPO2 to re-fit the pulsar spin frequency and orbital parameters. The pulsar is

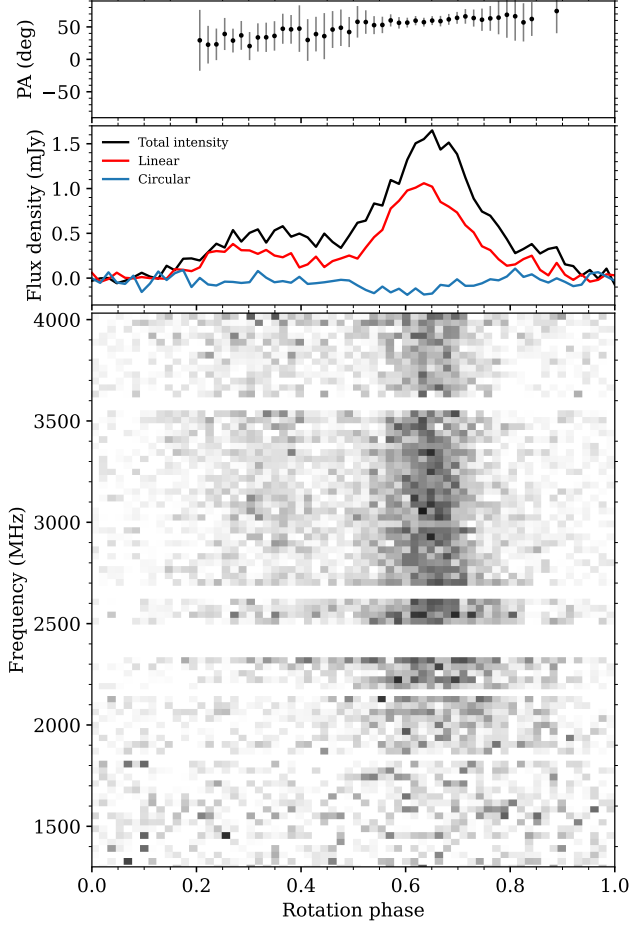


Figure 2. Linear polarization position angle swing (top), time and frequency averaged polarization profile (middle) and the total intensity spectrum (bottom) of PSR J1744–2946. Note, the average profile in the middle panel excluded data below 1900 MHz.

in a circular orbit with a period of 4.8 hr about a companion of mass $> 0.05 M_{\odot}$. Details of the pulsar and binary parameters are given in Table 1. Figure 1 shows the timing residuals both with and without the full timing model presented in Table 1 being subtracted from the ToAs. A small delay is apparent in the ToAs near orbital phase 0.25, which could be due to interactions with material being ablated off the companion. However, we find no evidence of radio eclipses or flux density variability at any part of the orbit.

Spectropolarimetric analysis was conducted using PSRCHIVE (Hotan et al. 2004; van Straten & Bailes 2011) where a Faraday rotation measure (RM) of $3011 \pm 3 \text{ rad m}^{-2}$ was recovered. This is the sixth largest absolute RM of any pulsar found to date. In Figure 2, we present both the polarization profile of PSR J1744–2946 and its rotational phase resolved radio spectrum after averaging together the observations taken on 2024 April 1 and 3. Its average profile is highly polarized with a linear fraction of 58 percent, with a largely flat position angle sweep across the profile.

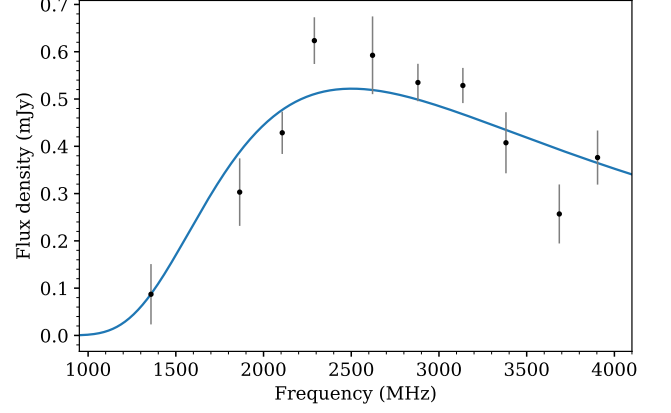


Figure 3. Flux density of PSR J1744–4429 as a function of observing frequency. Over-plotted in blue is our best-fit spectral model.

We obtained a refined DM by splitting the data between 2880–4032 MHz into 128 MHz subbands and then fitting the resulting multi-frequency ToAs using TEMPO2, yielding an improved $\text{DM} = 673.7 \pm 0.1 \text{ pc cm}^{-3}$. The pulsar is scatter broadened by multi-path radio wave propagation in the interstellar medium, to the point where it is not detected below ~ 1500 MHz. Fitting the profile at 2.6 GHz with a noise-free template generated from the 4 GHz profile convolved with an exponential tail returned a scattering timescale of $0.87 \pm 0.08 \text{ ms}$. Under a f^{-4} frequency scaling relation, this would correspond to a scattering timescale of $\sim 40 \text{ ms}$ at 1 GHz, less than a factor 2 from the scattering-DM relationship discussed in Cordes et al. (2022).

Flux densities are difficult to obtain due to both the effects of scatter-broadening and the wide pulse profile. We divided the band into 14 subbands and measured the flux density in each band by simply summing the values across all phase-bins. The lowest four bands have flux densities consistent with zero. Figure 3 shows the phase-averaged flux density as a function of observing frequency over-plotted with a fit to a power-law plus low-frequency turnover (see equation 17 in Jankowski et al. 2018).

4. DISCUSSION

The discovery of PSR J1744–2946 tentatively confirms the pulsar nature of the radio point source G359.13142–0.2000 identified by Yusef-Zadeh et al. (2024). However, the 2.5 arcmin half-width half-maximum beam of Murriyang at 4 GHz and our presently limited timing baseline preclude a definitive association. For a DM of $673.3 \text{ cm}^{-3} \text{ pc}$ in the direction of the Snake, the YMW16 (Yao et al. 2017) and NE2001 (Cordes & Lazio 2002) electron column density models for the Galaxy yield distance estimates of 4.6 and 8.4 kpc respectively. While DM distances should be treated with caution, particularly for the inner Galaxy, the larger NE2001 distance is consistent with a

lower-bound of ~ 8 kpc to the Snake inferred via H I absorption (Uchida et al. 1992). The DM of PSR J1744–2946 is noticeably lower than those of other pulsars in the vicinity of the Galactic Center which are typically $> 1000 \text{ cm}^{-3}\text{pc}$. Its high RM aligns well with the RM measured in the Snake itself (Gray et al. 1995), but is an order of magnitude lower than other pulsars in the Galactic Center (Schnitzeler et al. 2016; Shannon & Johnston 2013).

The pulsar has a very broad profile which appears to fill most of the 360° of rotational longitude. While many MSPs have broad profiles (Spiewak et al. 2022) these are usually composed of many different separate components rather than the two co-joined components seen here. The high degree of linear polarization is typical of MSPs with high \dot{E} values.

The spectrum of the pulsar displayed in Figure 3 is peculiar, particularly the spectral turn-over near 2.5 GHz. We note that although our flux density measurement at 4 GHz coincides with that of G359.13142–0.2000 in Yusef-Zadeh et al. (2024), their spectral index of -2.7 above 4 GHz is considerable steeper than the value of -2.0 that we measure below 4 GHz. For most pulsars, the spectral turnover occurs below ~ 100 MHz, although there exists a class of pulsars with turnovers near 1 GHz (Kijak et al. 2017), thought to be linked to free-free absorption in their nearby environment (Lewandowski et al. 2015). If assume a free-free absorption model and a PWN of size 0.1 pc with electron column density of 1000 cm^{-3} , then the emission measure would be $10^5 \text{ cm}^{-6}\text{pc}$ which would imply a relatively low electron temperature (< 100 K). This would mean the PWN contributes $100 \text{ cm}^{-3}\text{pc}$ to the pulsar DM, already uncomfortably large and places an upper limit on the magnetic field of $\sim 30 \mu\text{G}$ if the entirety of the pulsar RM arises in the PWN. This is a factor of two lower than that estimated for the Snake by Gray et al. (1995).

The presence of a luminous X-ray PWN in addition to a long ‘tail’ pointing back towards the Snake led Yusef-Zadeh et al. (2024) to suggest they are a result of a fast moving pulsar ($V > 500 \text{ kms}^{-1}$) with $\dot{E} > 10^{36} \text{ ergs}^{-1}$. In addition, although the X-ray luminosity is comparable with other PWN/PSR combinations listed in Hsiang & Chang (2021), all but one of the pulsars in their list are young with spin periods of 50 ms and above. The only MSP with a known X-ray PWN is PSR J2124–3358 (Romani et al. 2017), but its X-ray luminosity is only $10^{29} \text{ ergs}^{-1}$ and its velocity only 100 kms^{-1} . Theoretical work by Barkov & Lyutikov (2019) suggests that the relativistic outflow from a high \dot{E} pulsar

channeled along magnetic filaments is powering the luminosity of the Snake and causing the brightness enhancement in the kink. Both observational and theoretical evidence therefore appear at odds with our discovery of an MSP. With a spin-period of 8.4 ms, PSR J1744–2946 is unlikely to have $\dot{E} > 10^{36} \text{ ergs}^{-1}$ unless its period derivative (\dot{P}) is 10^3 times larger than expected from the bulk population and therefore by far the highest known for any MSP.

In summary, we have discovered the first MSP in the Galactic Center. In spite of the pulsar’s relatively high radio luminosity, a combination of free-free absorption and scattering renders the pulsations invisible below 2 GHz. Future surveys of the entire Galactic Center region at 3 GHz and above are therefore warranted. Detection of a large population of MSPs would lend support to the idea that the Fermi GeV excess in this region arises from such a population.

Although the expectations that G359.13142–0.2000 contains a pulsar appear to be borne out, PSR J1744–2946 is unexpectedly a binary millisecond pulsar with a relatively slow spin period of 8.4 ms. Its DM and RM appear to place it in the Galactic Center and its flux density matches with that of G359.13142–0.2000 at 4 GHz. However, it is difficult to reconcile the pulsar parameters with the spin-down energy required to power both the PWN and the Snake itself unless its \dot{P} is extraordinarily high. Further timing of the pulsar will yield both an accurate position and a \dot{P} in the near future.

We are grateful to CSIRO staff, especially Jane Kaczmarek and Lawrence Toomey, for helping support our observations. We thank Saurav Mishra for suggestions on pulsar searching and Juntao Bai for the code to compute scattering times. Murriyang, the Parkes radio telescope, is part of the Australia Telescope National Facility (<https://ror.org/05qajvd42>) which is funded by the Australian Government for operation as a National Facility managed by CSIRO. We acknowledge the Wiradjuri people as the traditional owners of the Observatory site. This project was supported by resources and expertise provided by CSIRO IMT Scientific Computing.

Facilities: Parkes/Murriyang

Software: DSPSR (van Straten & Bailes 2011) PRESTO (Ransom 2011) PSRCHIVE (Hotan et al. 2004; van Straten et al. 2012) TEMPO2 (Hobbs et al. 2006)

REFERENCES

- Barkov, M. V., & Lyutikov, M. 2019, MNRAS, 489, L28, doi: [10.1093/mnras/slz124](https://doi.org/10.1093/mnras/slz124)
- Bartels, R., Krishnamurthy, S., & Weniger, C. 2016, PhRvL, 116, 051102, doi: [10.1103/PhysRevLett.116.051102](https://doi.org/10.1103/PhysRevLett.116.051102)

- Cordes, J. M., & Lazio, T. J. W. 2002, arXiv e-prints, astro, doi: [10.48550/arXiv.astro-ph/0207156](https://doi.org/10.48550/arXiv.astro-ph/0207156)
- Cordes, J. M., Ocker, S. K., & Chatterjee, S. 2022, ApJ, 931, 88, doi: [10.3847/1538-4357/ac6873](https://doi.org/10.3847/1538-4357/ac6873)
- Deneva, J. S., Cordes, J. M., & Lazio, T. J. W. 2009, ApJL, 702, L177, doi: [10.1088/0004-637X/702/2/L177](https://doi.org/10.1088/0004-637X/702/2/L177)
- Eatough, R. P., Falcke, H., Karuppusamy, R., et al. 2013, Nature, 501, 391, doi: [10.1038/nature12499](https://doi.org/10.1038/nature12499)
- Gray, A. D., Cram, L. E., Ekers, R. D., & Goss, W. M. 1991, Nature, 353, 237, doi: [10.1038/353237a0](https://doi.org/10.1038/353237a0)
- Gray, A. D., Nicholls, J., Ekers, R. D., & Cram, L. E. 1995, ApJ, 448, 164, doi: [10.1086/175949](https://doi.org/10.1086/175949)
- Heywood, I., Rammala, I., Camilo, F., et al. 2022, ApJ, 925, 165, doi: [10.3847/1538-4357/ac449a](https://doi.org/10.3847/1538-4357/ac449a)
- Hobbs, G., Manchester, R. N., Dunning, A., et al. 2020, PASA, 37, e012, doi: [10.1017/pasa.2020.2](https://doi.org/10.1017/pasa.2020.2)
- Hobbs, G. B., Edwards, R. T., & Manchester, R. N. 2006, MNRAS, 369, 655, doi: [10.1111/j.1365-2966.2006.10302.x](https://doi.org/10.1111/j.1365-2966.2006.10302.x)
- Hotan, A. W., van Straten, W., & Manchester, R. N. 2004, PASA, 21, 302, doi: [10.1071/AS04022](https://doi.org/10.1071/AS04022)
- Hsiang, J.-Y., & Chang, H.-K. 2021, MNRAS, 502, 390, doi: [10.1093/mnras/stab025](https://doi.org/10.1093/mnras/stab025)
- Jankowski, F., van Straten, W., Keane, E. F., et al. 2018, MNRAS, 473, 4436, doi: [10.1093/mnras/stx2476](https://doi.org/10.1093/mnras/stx2476)
- Johnston, S., Kramer, M., Lorimer, D. R., et al. 2006, MNRAS, 373, L6, doi: [10.1111/j.1745-3933.2006.00232.x](https://doi.org/10.1111/j.1745-3933.2006.00232.x)
- Kijak, J., Basu, R., Lewandowski, W., Rożko, K., & Dembska, M. 2017, ApJ, 840, 108, doi: [10.3847/1538-4357/aa6ff2](https://doi.org/10.3847/1538-4357/aa6ff2)
- Lazarević, S., Filipović, M. D., Dai, S., et al. 2023, arXiv e-prints, arXiv:2312.06961, doi: [10.48550/arXiv.2312.06961](https://doi.org/10.48550/arXiv.2312.06961)
- Lewandowski, W., Rożko, K., Kijak, J., & Melikidze, G. I. 2015, ApJ, 808, 18, doi: [10.1088/0004-637X/808/1/18](https://doi.org/10.1088/0004-637X/808/1/18)
- Lower, M. E., Shannon, R. M., Johnston, S., & Bailes, M. 2020, ApJL, 896, L37, doi: [10.3847/2041-8213/ab9898](https://doi.org/10.3847/2041-8213/ab9898)
- O’Leary, R. M., Kistler, M. D., Kerr, M., & Dexter, J. 2015, arXiv e-prints, arXiv:1504.02477, doi: [10.48550/arXiv.1504.02477](https://doi.org/10.48550/arXiv.1504.02477)
- Pfahl, E., & Loeb, A. 2004, ApJ, 615, 253, doi: [10.1086/423975](https://doi.org/10.1086/423975)
- Ploeg, H., Gordon, C., Crocker, R., & Macias, O. 2020, JCAP, 2020, 035, doi: [10.1088/1475-7516/2020/12/035](https://doi.org/10.1088/1475-7516/2020/12/035)
- Ransom, S. 2011, PRESTO: Pulsar Exploration and Search Toolkit, Astrophysics Source Code Library, record ascl:1107.017. <http://ascl.net/1107.017>
- Rea, N., Esposito, P., Pons, J. A., et al. 2013, ApJL, 775, L34, doi: [10.1088/2041-8205/775/2/L34](https://doi.org/10.1088/2041-8205/775/2/L34)
- Romani, R. W., Slane, P., & Green, A. W. 2017, ApJ, 851, 61, doi: [10.3847/1538-4357/aa9890](https://doi.org/10.3847/1538-4357/aa9890)
- Schnitzeler, D. H. F. M., Eatough, R. P., Ferrière, K., et al. 2016, MNRAS, 459, 3005, doi: [10.1093/mnras/stw841](https://doi.org/10.1093/mnras/stw841)
- Shannon, R. M., & Johnston, S. 2013, MNRAS, 435, L29, doi: [10.1093/mnras/slt088](https://doi.org/10.1093/mnras/slt088)
- Spiewak, R., Bailes, M., Miles, M. T., et al. 2022, PASA, 39, e027, doi: [10.1017/pasa.2022.19](https://doi.org/10.1017/pasa.2022.19)
- Uchida, K., Morris, M., & Yusef-Zadeh, F. 1992, AJ, 104, 1533, doi: [10.1086/116337](https://doi.org/10.1086/116337)
- van Straten, W., & Bailes, M. 2011, PASA, 28, 1, doi: [10.1071/AS10021](https://doi.org/10.1071/AS10021)
- van Straten, W., Demorest, P., & Osłowski, S. 2012, Astronomical Research and Technology, 9, 237, doi: [10.48550/arXiv.1205.6276](https://doi.org/10.48550/arXiv.1205.6276)
- Yao, J. M., Manchester, R. N., & Wang, N. 2017, ApJ, 835, 29, doi: [10.3847/1538-4357/835/1/29](https://doi.org/10.3847/1538-4357/835/1/29)
- Yusef-Zadeh, F., Arendt, R. G., Wardle, M., Heywood, I., & Cotton, W. 2022, MNRAS, 517, 294, doi: [10.1093/mnras/stac2415](https://doi.org/10.1093/mnras/stac2415)
- Yusef-Zadeh, F., Zhao, J.-H., Arendt, R., et al. 2024, MNRAS, doi: [10.1093/mnras/stae549](https://doi.org/10.1093/mnras/stae549)